

# NUMERICAL INVESTIGATION OF FUSELAGE-STABILIZER-CONTROL SURFACE INTERFERENCE FOR A HYPERSONIC WAVERIDER VEHICLE

Xiaopeng LI, Wenping SONG, Zhonghua HAN

National Key Laboratory of Science and Technology on Aerodynamic Design and Research, Northwestern Polytechnical University, Xi'an, 710072, China

**Keywords:** *hypersonic waverider vehicle; stabilizer; control surface; interference*

## Abstract

*In this paper, the interference characteristics and mechanism among the fuselage-stabilizer-control surface which affect the efficiency of the control surface is studied through numerical simulation. The influence of fuselage and stabilizer (including the horizontal distance and vertical distance between the stabilizer and control surface) on the control surface efficiency is exposed and the interference mechanism is revealed. According to the simulation results, some conclusions can be drawn: (1) the existence of the waverider vehicle's fuselage, the existence of stabilizer, and the horizontal and vertical distance between stabilizer and control surface will affect the control surface efficiency; (2) by analyzing the flow interference mechanism, we find that the fuselage's lower Mach number region, the trailing-edge wake, the shock waves and tip vortex wake of the stabilizer, have a negative influence on the control surface. The influence of fuselage's lower Mach number region and the trailing-edge wake are stronger than that of shock waves and tip vortex wake of the stabilizer; (3) through the detailed analysis of the flow patterns, we get the following guidance for the waverider vehicle's layout design: in order to reduce the negative interference on the horizontal control surface efficiency, the horizontal control surface should be mounted in a position away from the stabilizer's trailing-edge wake as far as possible.*

## 1 Introduction

Waverider configurations have been extensively used on the hypersonic vehicles due to their advantage of achieving higher lift-to-drag ratio[1] [2] than other configurations. However, when the forebody of a waverider configuration produces a high lift which dominates the total lift[3], the stability margin is decreased[4] [5]. In order to increase a waverider's stability margin, a stabilizer can be installed in front of the control surface, which results in complicated interference among the fuselage, stabilizer and control surface. When a stabilizer is installed in front of a control surface, it has a negative influence on the control surface. The investigation of the interference characteristics among the fuselage, stabilizer and control surface will be helpful to the design of fuselage-stabilizer-control surface combination, especially for the efficiency improvement of a control surface.

In this paper, the interference mechanism among the fuselage-stabilizer-control surface combination is studied through numerical simulation. The influence of the fuselage and stabilizer on the efficiency of the control surface is investigated and the interference mechanism is shown by analyzing the wave patterns, vortex wake, total pressure loss in the region between stabilizer and control surface. Some conclusions can be drawn: (1) the existence of the waverider vehicle's fuselage, the existence of stabilizer, and the horizontal and vertical distance between stabilizer and control surface will affect the control surface efficiency; (2) by analyzing the flow interference mechanism, we find that the fuselage's lower Mach number region, the trailing-edge wake, the shock waves and tip vortex wake of the stabilizer, have a negative

influence on the control surface. The influence of fuselage's lower Mach number region and the trailing-edge wake are larger than that of shock waves and tip vortex wake of the stabilizer; (3) through the detailed analysis of the flow patterns, we get the following guidance for the waverider vehicle's layout design: in order to reduce the negative interference on the horizontal control surface efficiency, the horizontal control surface should be mounted in a position away from the stabilizer's trailing-edge wake as far as possible.

The outcome of this research is of significant reference value for design of the waverider configuration.

## 2 Solution Methodology

### 2.1 Numerical Method

The compressible 3-D Reynolds-averaged Navier-Stokes (RANS) equations are solved using finite volume method. The total variation diminishing (TVD) scheme based on Riemann solver and a new multidimensional interpolation framework are used for spatial discretization. The implicit local time-stepping scheme is adopted for the time integration. The  $k-\omega$  SST turbulence model is used to satisfy the requirement of turbulence closure. The multi-block method based on the structured grids and MPI parallel computing strategy is also used to accelerate the computation. The no slip velocity and adiabatic boundary conditions on the wall are imposed to the solution.

### 2.2 Validation of Numerical Method

For the purposes of evaluating numerical method, cases have been selected from the available experimental database [6] of non-axisymmetric missile configurations compiled by NASA Langley research center. These wind-tunnel tests were conducted in the NASA Langley unitary plan wind Tunnel. Fig.1.(a) shows the computational model of square cross-section body with four tail fins, the width of the sides of the square body is 93.98mm, and the length of the missile is 1221.74mm. The multi-block structured grids were generated by the

ICEM-CFD software, shown in Fig. 1.(b). Fig. 2. shows the comparison of normal force and pitching moment coefficients between computational data and wind tunnel experimental data of the missile configuration at the free-stream condition of  $Ma=4.5$ ,  $Re=1.312 \times 10^7$ . The computational results show good agreement with the experimental data.

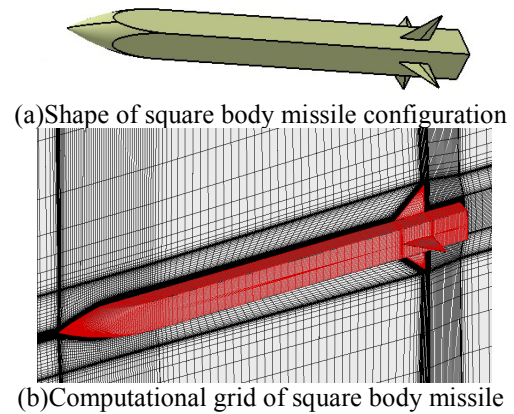


Fig. 1. Shape of square missile and computational grid

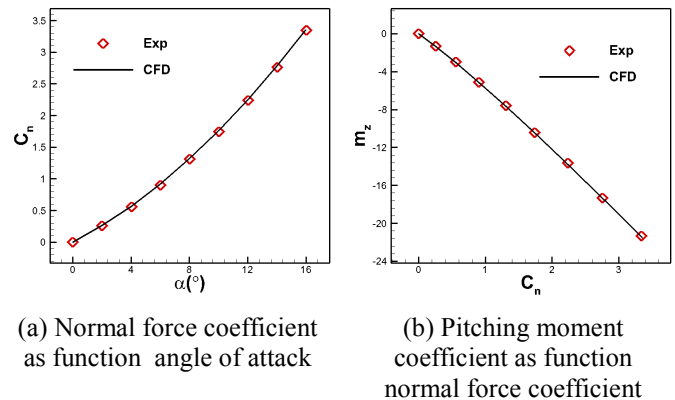


Fig. 2. Comparison of measured and computed aerodynamic coefficients for square body missile

## 3 Computational Models and Grids

Three models are investigated in present paper, the isolated control surface, the fuselage/control surface configuration and the fuselage-stabilizer-control surface configuration. Fig. 3(a) shows the computational model of isolated control surface, the root chord length of control surface is 0.6m, the tip chord length of control surface is 0.3m, the span of control surface is 0.24m, the leading edge sweep angle is  $55^\circ$ . Fig. 3(b) and Fig. 3 (c) show the computational models of fuselage-stabilizer and fuselage-stabilizer-control surface configuration, respectively. The multi-block structured grids

## NUMERICAL INVESTIGATION OF FUSELAGE-STABILIZER-CONTROL SURFACE INTERFERENCE FOR A HYPERSONIC WAVEDIDER VEHICLE

were generated by the software ICEM-CFD. Fig. 4. shows oblique side view of the surface grids of the fuselage-stabilizer-control surface configuration, and the half model's grids consisted of approximately 8-million cells. Calculations were performed at Mach number 6, angle of attack  $4^\circ$ , Reynolds number of 4 million based on the mean aerodynamic chord of the control surface.

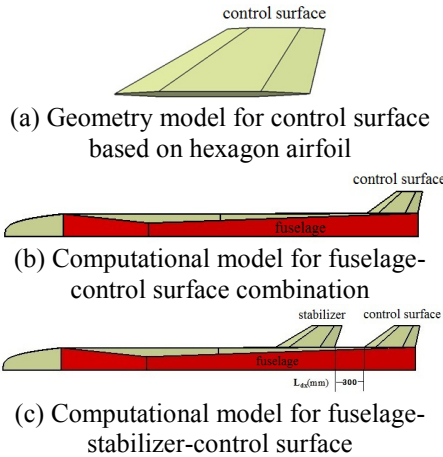


Fig. 3. The model geometry for fuselage-stabilizer-control surface combination

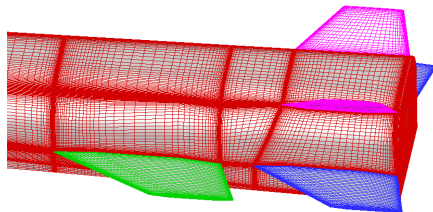


Fig. 4. Surface grids of the fuselage-stabilizer-control surface configuration

### 4 Results and Discussion

Based on Reynolds-averaged Navier-Stokes equations simulations, the hypersonic flow around control surface, fuselage-control surface, fuselage-stabilizer-control surface have been numerically simulated to study interference mechanism between control surface, stabilizer and fuselage. The remainder of this paper is outlined as follows. Section 4.1 summarizes the interference characteristics between control surface and fuselage, stabilizer and control surface. Section 4.2 shows the influence of the horizontal and vertical distance between the stabilizer and control surface on the control surface efficiency. Section 4.3 reveals the interference mechanism in the junction region between stabilizer and control surface,

meanwhile, figures out the quantitative effects by fuselage's lower Mach number region, stabilizer's trailing-edge wake and shock waves.

#### 4.1 Interference Characteristics among Fuselage, Stabilizer and Control surface

In order to reveal the interference characteristics between control surface and fuselage, the hypersonic flows around isolated control surface and fuselage-control surface combination configuration have been numerically simulated respectively. The flow difference between the control surface with and without fuselage is found out. Fig. 5 shows pressure contours on the lower side of control surface with and without fuselage. Fig. 5.(a) shows the lower side pressure contours of the isolated control surface; Fig. 5.(b) shows pressure contours on the lower side of the control surface of fuselage-control surface configuration. By comparison, we found the pressure of the root part of the lower side surface was reduced by the fuselage. Fig. 6. shows the pressure contours around the fuselage and control surface in the crossflow section. The effects of fuselage on the pressure of the root part of the lower side of the control surface are also can be seen clearly. Fig. 7. shows the Mach number contours on the yaw plane which through the leading edge of the control surface for the fuselage-control surface configuration. We can see obviously that the local Mach number of the flow near the fuselage region is reduced significantly due to the fuselage's boundary layer. The strong interference of fuselage on the root part of the control surface reveals the same interference mechanism as Fig. 5. and Fig.6.

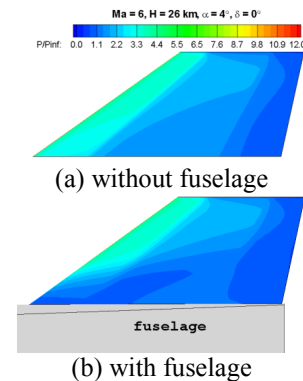


Fig. 5. Pressure contours on the lower side of control surface

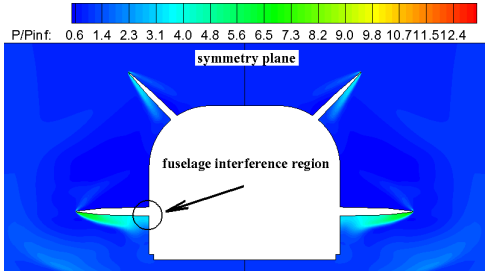


Fig. 6. Pressure contours around fuselage and control surface in crossflow plane

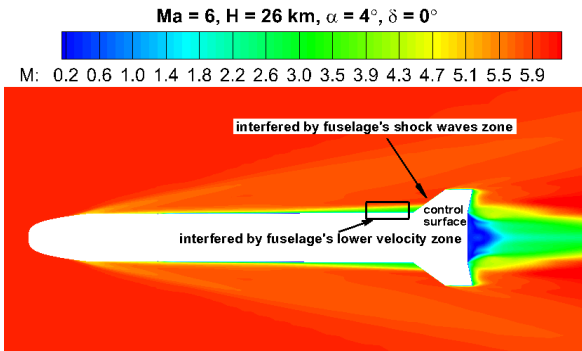


Fig. 7. Mach number contours on the yaw plane

Fig. 8. shows the comparison of Mach number contours on the yaw plane for fuselage-control surface and fuselage-stabilizer-control surface configuration. Due to the presence of stabilizer, the Mach number of control surface's root part is slightly increased, thus the interference caused by the fuselage's lower Mach number zone is weakened. From semi-span to tip region, the control surface is mainly interfered by stabilizer's trailing-edge wake and shock waves.

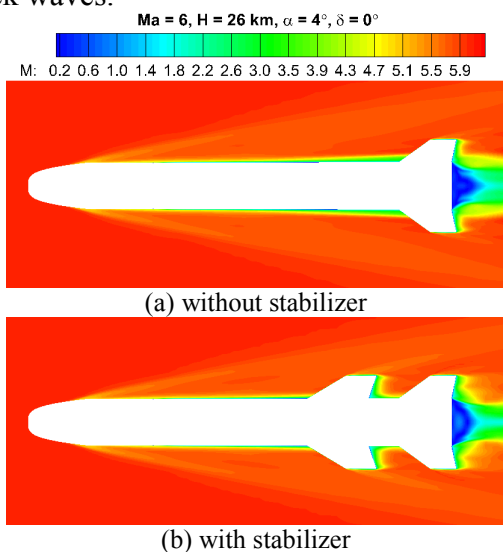


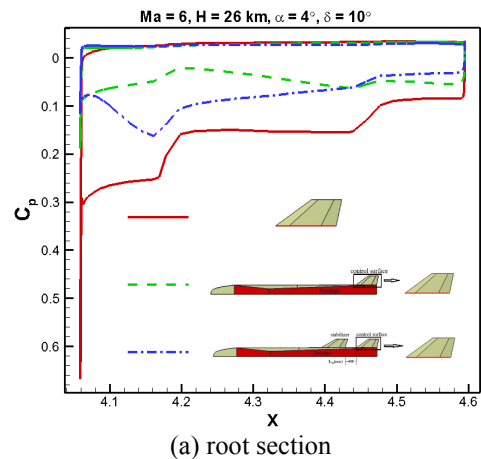
Fig. 8. Comparison of Mach number contours on the yaw plane

Fig. 9. shows the pressure distributions of the control surface in the root, semi-span and tip sections of three investigated configurations, including the isolated control surface, the control surface of fuselage-control surface configuration and the control surface of fuselage-stabilizer-control surface configuration.

By comparing Fig. 8. and Fig. 9.(a), the strong interference of fuselage on the root part of the control surface of fuselage-control surface configuration and the control surface of fuselage-stabilizer-control surface configuration is shown from Mach number contours on the yaw plane and the pressure distributions. Due to the presence of stabilizer, the interference caused by the fuselage is weakened.

By comparing Fig. 8. and Fig. 9.(b), we can see that the semi-span sections of the fuselage-control surface configuration and the fuselage-stabilizer-control surface configuration are mainly interfered by the shock waves of fuselage. Compared with the pressure distribution of the isolated control surface, the interference caused by the shock waves is weaker than that of the fuselage. Due to the presence of stabilizer, the interference caused by the stabilizer's trailing edge wakes tends to reduce the pressure on the lower control surface.

By comparing Fig. 8. and Fig. 9.(c), we found that the tip section of the fuselage-control surface configuration is scarcely interfered by the fuselage's shock waves. For the fuselage-stabilizer-control surface configuration, due to the presence of stabilizer, the control surface's lower side pressure is decreased by the interference caused by the stabilizer trailing edge wakes.



(a) root section

**NUMERICAL INVESTIGATION OF FUSELAGE-STABILIZER-CONTROL SURFACE INTERFERENCE FOR A HYPERSONIC WAVEDIDER VEHICLE**

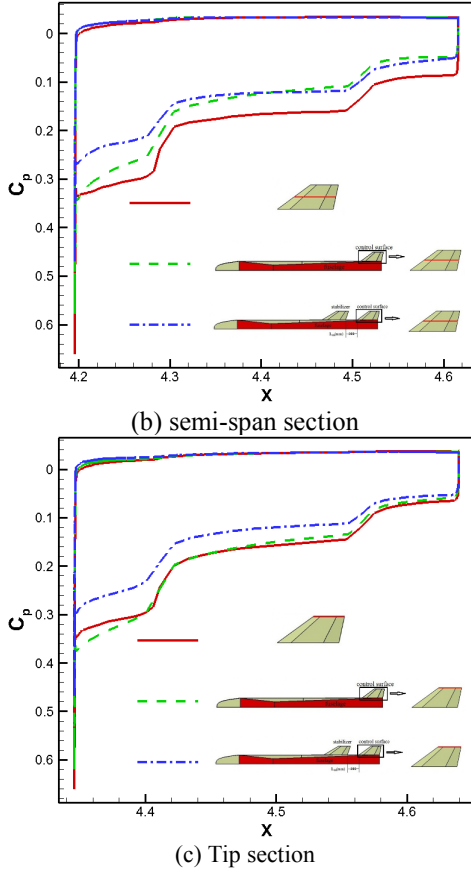


Fig. 9. The pressure distributions of the control surface's root, semi-span, tip section

**4.2 The Influence of Horizontal and Vertical Distance between the Stabilizer and Control surface on the Control Surface Efficiency**

In this sub-section, the influence of the horizontal and vertical distance between the stabilizer and control surface on the control surface efficiency is given. Fig. 10 shows the horizontal distance of  $L_{dx} = 900\text{mm}$ ,  $300\text{mm}$ ,  $100\text{mm}$  between the stabilizer and control surface respectively (corresponding to vertical distance  $L_{dy}$  is  $0\text{mm}$ ).

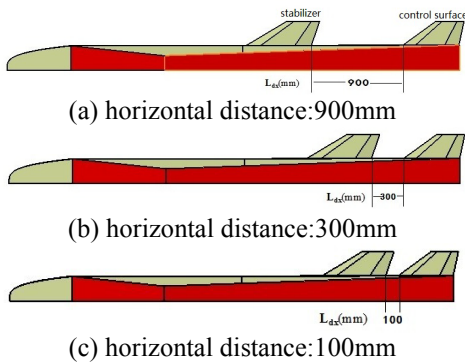


Fig. 10. The horizontal distance between the stabilizer and the control surface

The control surface efficiency is defined as :

$$m_z^\delta = \frac{m_{z,\delta 1} - m_{z,\delta 0}}{\delta 1 - \delta 0} \quad (1)$$

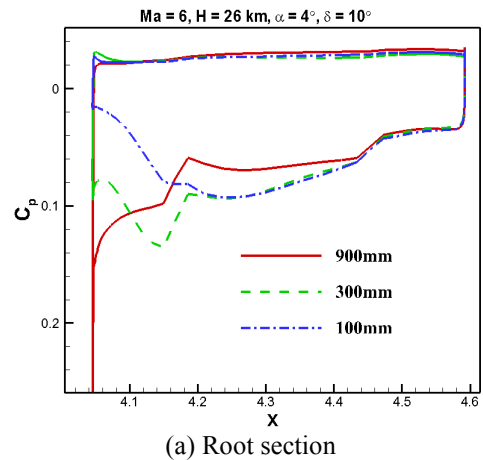
where  $m_{z,\delta 1}$  is the pitching moment coefficient of the control surface at the deflection of  $10^\circ$ ,  $m_{z,\delta 0}$  is the pitching moment coefficient of the control surface at the deflection of  $0^\circ$ .

Table 1. shows the control efficiencies of different horizontal distance between stabilizer and control surface. The efficiency is decreased with the horizontal distance shortened.

Tab.1. The control surface efficiency of different  $L_{dx}$

The horizontal distance between stabilizer and control surface ( $L_{dy}=0\text{mm}$ )	Control efficiency	$\Delta\%$
900mm	0.0418	0%
300mm	0.0378	-9.5%
100mm	0.0363	-13.2%

Fig. 11. shows the pressure distributions of the control surface in the root, semi-span and tip sections of the configurations with the horizontal distance of  $L_{dx} = 900\text{mm}$ ,  $300\text{mm}$ ,  $100\text{mm}$  between the stabilizer and control surface. In general, decreasing the horizontal distance between stabilizer and control surface causes a decrease in the pressure on the lower side of control surface.



(a) Root section

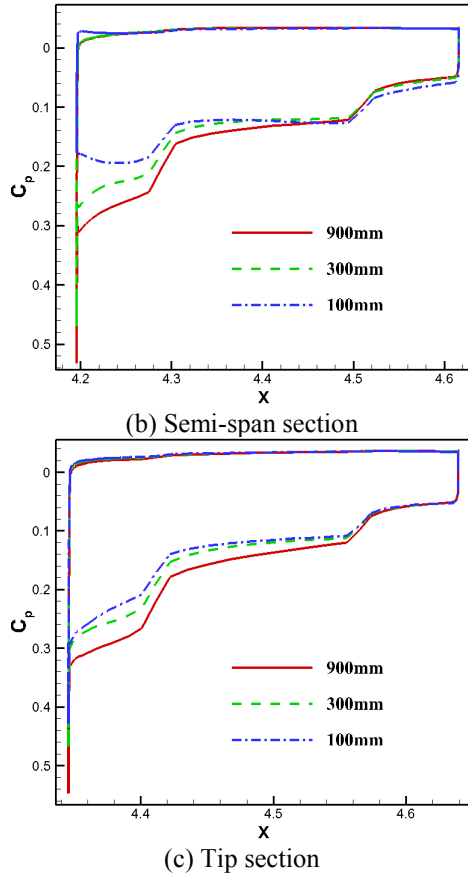


Fig. 11. The pressure distribution of the control surface's root, semi-span, tip section

Fig. 12. shows the vertical distance parameters of  $L_{dy}$  for the stabilizer and control surface.  $L_{dy}=40\text{mm}$  indicates that the stabilizer is moved up 40mm from the initial location ( $L_{dy}=0\text{mm}$ ),  $L_{dy}=-40\text{mm}$  indicates that the stabilizer is moved down 40mm from the initial location (the three configurations' horizontal distance  $L_{dx}$  between the stabilizer and control surface is 300mm).

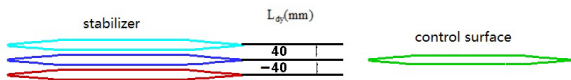


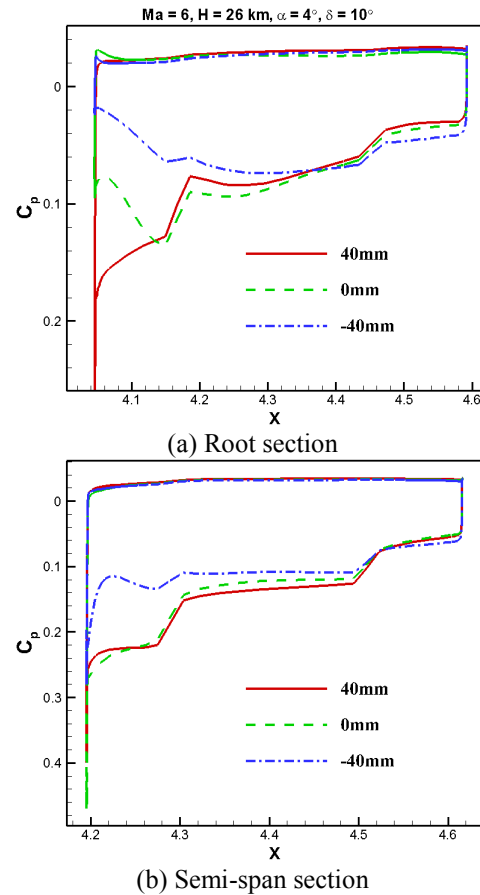
Fig. 12. The vertical distance parameters between stabilizer and control surface

Table 2. shows the control surface efficiency of the different vertical distance parameters for the stabilizer and control surface. Taking  $L_{dy}=0$  as reference, it is found that the control surface efficiency is increased by 5.3% with the vertical position of the stabilizer at  $L_{dy}=40\text{mm}$ , and is decreased by 11.9% with the vertical position of the stabilizer at  $L_{dy}=-40\text{mm}$ .

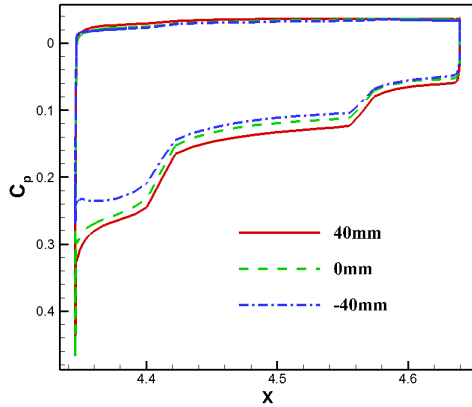
Tab. 2. The control surface efficiency of different  $L_{dy}$

The vertical distance parameters of stabilizer and control surface ( $L_{dx}=300\text{mm}$ )	Control efficiency	$\Delta\%$
0mm	0.0378	0%
40mm	0.0398	+5.3%
-40mm	0.0333	-11.9%

Fig. 13. shows the pressure distributions of the control surface in the root, semi-span and tip sections for the three configurations with the vertical position of the stabilizer at  $L_{dy}=-40\text{mm}$ , 0mm, 40mm. Taking  $L_{dy}=0$  as reference, it is found that the control surface's lower surface pressure is increased when  $L_{dy}=40\text{mm}$ , and decreased when  $L_{dy}=-40\text{mm}$ , which causes the increasing effect and decreasing effect on the control surface efficiency mentioned above.



**NUMERICAL INVESTIGATION OF FUSELAGE-STABILIZER-CONTROL SURFACE INTERFERENCE FOR A HYPERSONIC WAVEDIDER VEHICLE**



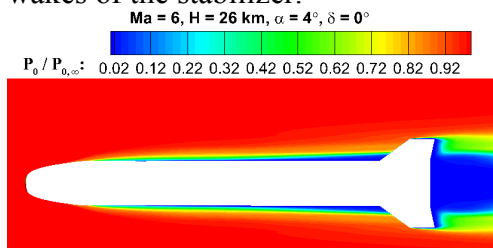
(c) Tip section

Fig. 13. The pressure distribution of the control surface's root, semi-span, tip section

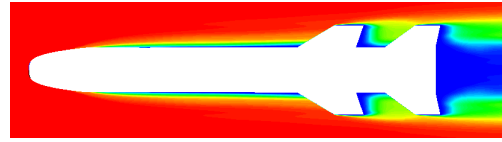
**4.3 Interference Mechanism and Quantitative Analysis of Interference**

The flow field characteristics illustrated by Mach number and pressure contours were shown in the above sub-sections, in order to reveal the interference mechanism of the complex flow field structure more deeply, both qualitative and quantitative results are presented and investigated in this section.

Fig. 14. shows the comparison of total pressure distributions on the yaw plane for the fuselage-control surface and the fuselage-stabilizer-control surface configurations. For the fuselage-control surface, the total pressure of control surface's root part is dramatically decreased due to the presence of fuselage. Away from the root part of the control surface, the total pressure is slightly decreased, indicating the interference caused by the fuselage is reduced. For the fuselage-stabilizer-control surface, due to the presence of stabilizer, the control surface's total pressure decrease near the root part caused by the fuselage is weakened, but away from the root part of the control surface, the total pressure is reduced more significantly than the fuselage-control surface configuration, which is caused by the trailing edge wakes of the stabilizer.



(a) without stabilizer



(b) with stabilizer

Fig. 14. Total pressure distribution on the yaw plane

Total pressure distribution in front of control surface is depicted in Fig. 15. It is shown clearly that near the tip section the control surface is interfered by the vortex wakes of the stabilizer. It also can be seen that away from the tip section the control surface is influenced by the trailing-edge wakes and shock waves of the stabilizer, which have a negative influence on the efficiency of the control surface.

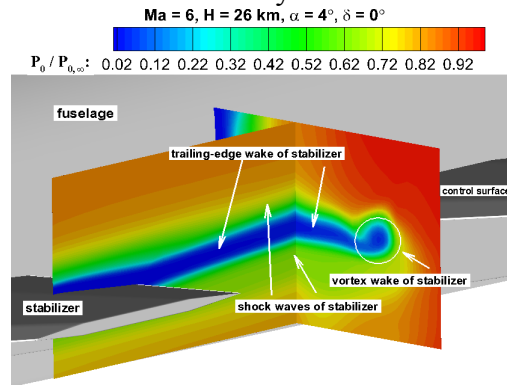


Fig. 15. Total pressure distributions in front of the control surface

Fig.16. shows the comparison of total pressure distributions in front of the control surface for the fuselage-control surface and the fuselage-stabilizer-control surface configuration. For the fuselage-control surface configuration, the total pressure of control surface's root part is significantly decreased due to the presence of fuselage. Away from the root part of the control surface, the total pressure is slightly decreased, indicating the interference caused by the fuselage is reduced. For the fuselage-stabilizer-control surface configuration, near the root part of the control surface, due to the presence of stabilizer, the total pressure loss caused by the fuselage is less than that of fuselage-control surface configuration, whereas, away from the root part of the control surface, the total pressure is reduced more significantly than the fuselage-control surface configuration, which is caused by the trailing edge wakes of the stabilizer.

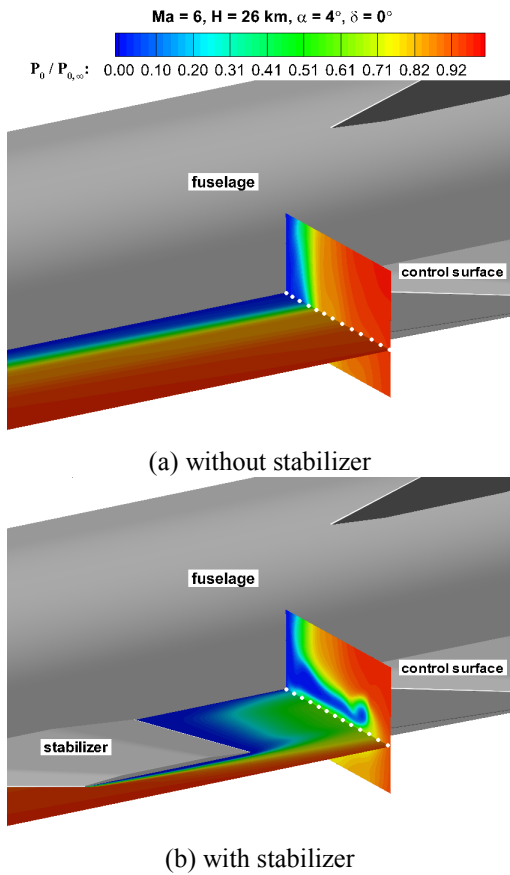


Fig.16. Total pressure distributions in front of the control surface

In order to quantitatively investigate the complex interactions in the junction region between the stabilizer and control surface, we introduce a new variable, the relative total pressure loss, for quantitative study of the interference characteristics. The relative total pressure loss  $C_{RTPL}$  is defined by

$$C_{RTPL} = 1 - \frac{P_0}{P_{0,\infty}} \quad (2)$$

where  $p_0$  is local total pressure,  $p_{0,\infty}$  is the total pressure of free stream.

Fig. 17. shows the relative total pressure loss in the spanwise direction of the fuselage-control surface and fuselage-stabilizer-control surface configuration, the values of the relative total pressure loss are chosen at the white discrete points which are shown in Fig.16. From the root part to 40% spanwise location, the total pressure loss in front of the control surface of the fuselage-control surface configuration is greater than that of the fuselage-stabilizer-control surface configuration, which reveals that the interaction of fuselage on the control surface

of the fuselage-control surface configuration is dominating one. From 40% spanwise location to tip part, the total pressure loss in front of the control surface of the fuselage-control surface configuration is less than that of the fuselage-stabilizer-control surface configuration, which reveals the interaction of the stabilizer on the control surface of the fuselage-stabilizer-control surface configuration is dominating one.

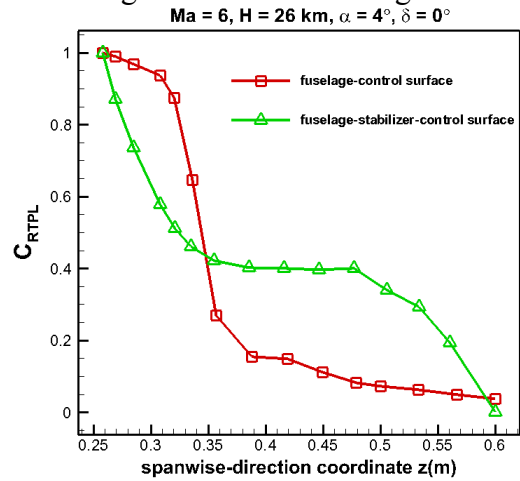


Fig. 17. The relative total pressure loss in front of the control surface in spanwise direction for three investigated configurations

Fig. 18. shows the total pressure distributions on semi-span of the stabilizer. It can be obviously seen that the trailing-edge wakes and shock waves of the stabilizer have a negative influence on the control surface.

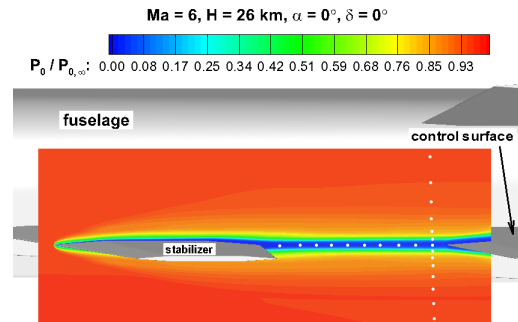


Fig. 18. The total pressure distribution on semi-span of stabilizer plane

Fig. 19. shows the relative total pressure loss in the streamwise direction behind the stabilizer. From the trailing-edge of stabilizer to leading-edge of the control surface on semi-span section plane, the values of the relative total pressure loss are chosen at the white discrete points which are shown in Fig. 18. The relative total pressure loss is within 3% in the horizontal direction, indicating that the relative

**NUMERICAL INVESTIGATION OF FUSELAGE-STABILIZER-CONTROL SURFACE INTERFERENCE FOR A HYPERSONIC WAVEDIDER VEHICLE**

total pressure loss is very small in the horizontal direction.

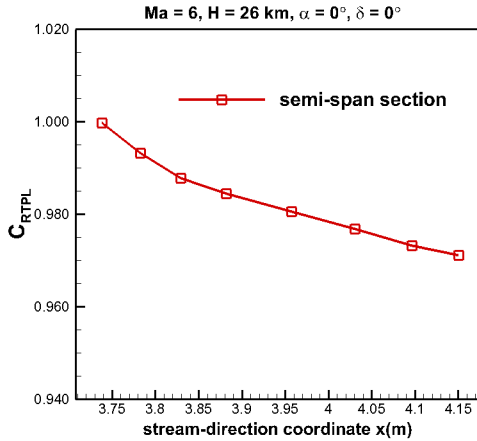


Fig. 19. The relative total pressure loss as function of streamwise-direction coordinate (x)

Fig. 20. shows the relative total pressure loss in the vertical direction in front of the control surface. From upper to lower position, the values of the relative total pressure loss are chosen at the white discrete points which are shown in Fig. 18. In the trailing-edge region of the stabilizer, the relative total pressure loss is large, the maximum  $C_{RTPL}$  reaches the high value of 95%. In the shock wave region, the relative total pressure loss is small,  $C_{RTPL}$  is less than 15%. It is can be concluded that the control surface should be mounted away from the stabilizer's trailing wake region to reduce the negative influence on the efficiency of the control surface.

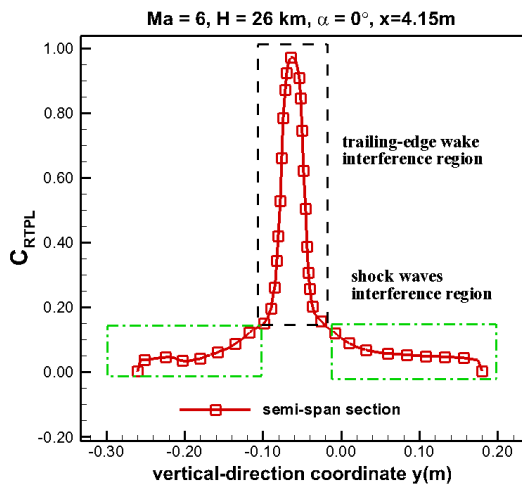


Fig. 20. The relative total pressure loss as function of vertical-direction coordinate (y)

Fig. 21. shows the total pressure distributions of the control surface's semi-span sections for the horizontal distance of  $L_{dx}$

=900mm, 300mm, 100mm between the stabilizer and control surface. By comparing the total pressure distributions, it is found that the more closely the control surface near the trailing edge wakes of the stabilizer, the more strongly the interference is, hence the more greatly the control surface efficiency decreases.

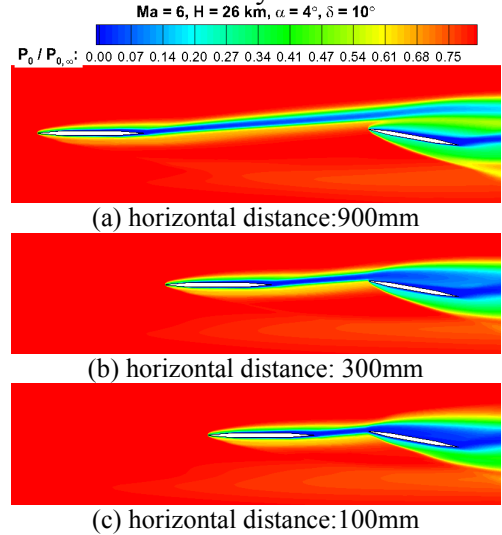


Fig. 21. The total pressure distribution of the control surface's root, semi-span, tip section

Fig. 22. shows the total pressure distributions of the control surface's semi-span sections for the different vertical distance parameters for the stabilizer and control surface. By comparing the total pressure distributions, we can also see clearly that when the control surface is mounted in a position the farther away from the stabilizer's trailing-edge wake region, the less the interference is, hence the higher the control surface efficiency is.

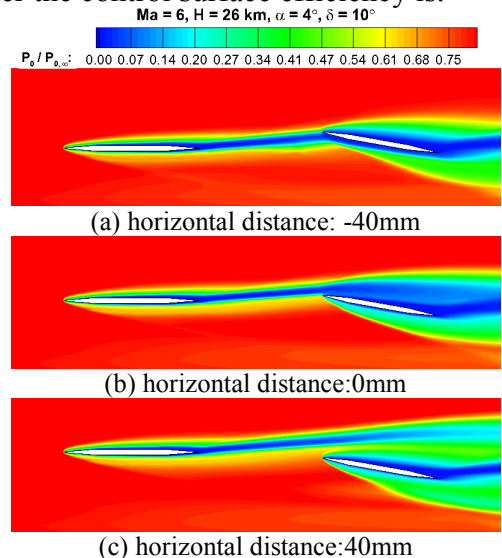


Fig. 22. The total pressure distribution of the control surface's root, semi-span, tip section

## 5 Conclusions

In this paper, the hypersonic flow around waverider-derived configurations has been numerically simulated by solving the RANS equations. The interference mechanism among fuselage, stabilizer and control surface is revealed, which provides a useful guidance to the design of a waverider-derived configuration. Some conclusions are drawn as follows:

- (1) The fuselage, stabilizer, and the horizontal and vertical distance between stabilizer and control surface will affect the control surface efficiency;
- (2) The fuselage's lower Mach number region, the trailing-edge wake, the shock waves and tip vortex wake of the stabilizer, have a negative influence on the control surface. The influence of fuselage's lower Mach number region and the trailing-edge wake are larger than that of shock waves and tip vortex wake of the stabilizer;
- (3) Through the detailed analysis of the flow patterns, we get the following guidance for the waverider vehicle's layout design: in order to reduce the negative interference on the horizontal control surface efficiency, the horizontal control surface should be mounted in a position away from the stabilizer's trailing-edge wake as far as possible.

## References

- [1] Norris J D. Mach 8 high Reynolds number static stability capability extension using a hypersonic waverider at AEDC funnel 9, AIAA Paper 2006-2815, 2006.
- [2] Ye Youda. Study on Aerodynamic Characteristics and Design Optimization for High Speed Near Space Vehicle. *Advances in Mechanics*, Vol. 39, No. 6, pp. 683-694, 2009.
- [3] Jackson D J. CFD Analysis of a Generic Waverider. AIAA Paper 2006-2817, 2006.
- [4] Zhang J, Wang F M. Hypersonic waverider aerodynamic performance studies. *Journal of Astronautics*, Vol. 28, No. 1, pp. 203-208, 2007.
- [5] Liu Zhen Xia, Xiao Hong. Numerical Simulation, Experiment and Optimization of Hypersonic Vehicle Configuration. *Journal of Astronautics*, Vol. 30, No. 3, pp. 411-421, 2009.
- [6] Birch T, Allen J, Wilcox F J. Force, Surface Pressure and Flowfield Measurements on a Slender Missile Configuration with Square Cross-Section at Supersonic Speeds. AIAA Paper 2004-5451, 2004.

## Contact Author Email Address

Xiaopeng Li: xiaopenglyy@126.com;

Wenping Song: wpsong@nwpu.edu.cn;

Zhonghua Han: hanzh@nwpu.edu.cn

## Copyright Statement

The authors confirm that they, and/or their company or organization, hold copyright on all of the original material included in this paper. The authors also confirm that they have obtained permission, from the copyright holder of any third party material included in this paper, to publish it as part of their paper. The authors confirm that they give permission, or have obtained permission from the copyright holder of this paper, for the publication and distribution of this paper as part of the ICAS 2014 proceedings or as individual off-prints from the proceedings.